

Superfluid phases and excitations in a cold gas of d-wave interacting bosonic atoms and molecules

Zehan Li(李泽汉), Jian-Song Pan, and W Vincent Liu

Citation: Chin. Phys. B, 2021, 30 (**6**): 066703. DOI: 10.1088/1674-1056/abd7d7
Journal homepage: http://cpb.iphy.ac.cn; http://iopscience.iop.org/cpb

What follows is a list of articles you may be interested in

Cluster mean-field study of spinor Bose-Hubbard ladder: Ground-state phase diagram and many-body population dynamics

Li Zhang(张莉), Wenjie Liu(柳文洁), Jiahao Huang(黄嘉豪), and Chaohong Lee(李朝红)
Chin. Phys. B, 2021, 30 (**2**): 026701. DOI: 10.1088/1674-1056/abd760

Generating two-dimensional quantum gases with high stability

Bo Xiao(肖波), Xuan-Kai Wang(王宣恺), Yong-Guang Zheng(郑永光), Yu-Meng Yang(杨雨萌), Wei-Yong Zhang(章维勇), Guo-Xian Su(苏国贤), Meng-Da Li(李梦达), Xiao Jiang(江晓), Zhen-Sheng Yuan(苑震生)
Chin. Phys. B, 2020, 29 (**7**): 076701. DOI: 10.1088/1674-1056/ab8ac8

Superfluidity of coherent light in self-focusing nonlinear waveguides

Ze Cheng(成泽)
Chin. Phys. B, 2017, 26 (**4**): 046701. DOI: 10.1088/1674-1056/26/4/046701

Landau damping in a dipolar Bose-Fermi mixture in the Bose-Einstein condensation (BEC) limit

S M Moniri, H Yavari, E Darsheshdar
Chin. Phys. B, 2016, 25 (**12**): 126701. DOI: 10.1088/1674-1056/25/12/126701

A space-dependent atomic superfluid current in Bose-Einstein condensates

Li Fei, Li Yong-Fan, Zhang Ping-Ke, Ai Zhen-Zhou, Wu Chang-Yi
Chin. Phys. B, 2015, 24 (**4**): 046701. DOI: 10.1088/1674-1056/24/4/046701

Superfluid phases and excitations in a cold gas of d-wave interacting bosonic atoms and molecules*

Zehan Li(李泽汉)[1], Jian-Song Pan[2,†], and W Vincent Liu[1,2,‡]

[1] Department of Physics and Astronomy, University of Pittsburgh, Pittsburgh, PA 15260, USA

[2] Wilczek Quantum Center, School of Physics and Astronomy and T. D. Lee Institute, Shanghai Jiao Tong University, Shanghai 200240, China

(Received 6 November 2020; revised manuscript received 22 December 2020; accepted manuscript online 4 January 2021)

Motivated by recent advances in orbitally tuned Feshbach resonance experiments, we analyze the ground-state phase diagram and related low-energy excitation spectra of a d-wave interacting Bose gas. A two-channel model with d-wave symmetric interactions and background s-wave interactions is adopted to characterize the gas. The ground state is found to have three interesting superfluid phases: atomic, molecular, and atomic–molecular. In great contrast to what was previously known about the p-wave case, the atomic superfluid is found to be momentum-independent for the d-wave case discussed here. The Bogoliubov spectra above each superfluid phase are obtained both analytically and numerically.

Keywords: d-wave interaction, quantum gas, Bogoliubov spectrum, superfluid

PACS: 67.85.−d, 03.75.Hh, 05.30.Jp **DOI:** 10.1088/1674-1056/abd7d7

1. Introduction

Orbital high-partial-wave interacting quantum gases[1] have steadily attracted research interest, due to their potential to show exotic superfluidity. For example, d-wave interacting Fermi gases may be compared with a d-wave superfluid. Recently, d-wave scattering resonance has been observed in more and more ultracold atomic gases.[2–6] In particular, the observation of degenerate d-wave-interacting Bose gases with d-wave shape resonance[5] makes the hidden d-wave many-body correlation more experimentally accessible.

Unlike s-wave interactions, the closed channels of high-partial-wave Feshbach resonance carry finite momentum. For example, the closed channels of the p-wave Feshbach resonance carry a total angular momentum of $1\hbar$ and the interaction term is proportional to the momentum k. It is predicted that a finite-momentum superfluid will emerge in a p-wave interacting Bose gas.[7–9] The closed channels of d-wave Feshbach resonance carry a total angular momentum of $2\hbar$, and hence the many-body form is proportional to the square of the momentum k^2. Although d-wave electronic Fermi superconductors have been extensively studied in condensed-matter physics, to the best of our knowledge, determination of the possible many-body states that a d-wave interacting atomic Bose gas can exhibit is an open question.

Inspired by recent experimental progress,[3,5,6] in this paper, we analyze the zero-temperature mean-field ground state and Bogoliubov spectrum of a d-wave interacting Bose gas. A two-channel model is adopted for a mixture of two components interacting via the d-wave interaction. Similarly to the p-wave interacting Bose gas,[7–9] the mean-field ground state typically has three quantum phases: atomic superfluid (ASF), molecular superfluid (MSF), and atomic–molecular superfluid (AMSF). However, unlike the p-wave case, the atomic superfluid does not carry finite momentum. The phase boundaries are analytically obtained. Furthermore, the Bogoliubov excitation spectrum is analyzed both numerically and analytically above the superfluid ground state with d-orbital aspects.

2. Model

Inspired by the experiments detailed in Refs. [3,10], we will focus on a gas mixture of two distinguishable bosonic atoms (e.g., ^{85}Rb and ^{87}Rb). The two atomic fields are created by $\hat{\psi}_\sigma^\dagger = (\hat{\psi}_1^\dagger, \hat{\psi}_2^\dagger)$ and interact through a d-wave FR associated with a tunable molecular bound state.[7,11] According to the symmetry of this system, the angular momentum is a good quantum number and the related d-wave molecule (e.g., ^{85}Rb–^{87}Rb) field is created by $\hat{\phi}_m^\dagger = (\hat{\phi}_{-2}^\dagger, \hat{\phi}_{-1}^\dagger, \hat{\phi}_0^\dagger, \hat{\phi}_1^\dagger, \hat{\phi}_2^\dagger)$, which corresponds to the five closed-channel molecular states (e.g., l_z=0, ±1, ±2). Apart from the d-wave interaction, we assume that the system is also subject to background atom–atom, molecule–molecule and atom–molecule s-wave interactions. The Hamiltonian density for this system is written as (we take $\hbar$=1 throughout)[12]

$$\mathcal{H} = \sum_{\sigma=1,2} \hat{\psi}_\sigma^\dagger \Big(-\frac{\nabla^2}{2m} - \mu_\sigma \Big) \hat{\psi}_\sigma + \sum_{m=-2}^{2} \Big[\hat{\phi}_m^\dagger \Big(-\frac{\nabla^2}{4m}$$

*Project supported by the AFOSR (Grant No. FA9550-16-1-0006), the MURI-ARO (Grant No. W911NF17-1-0323), the National Natural Science Foundation of China (Grant Nos. 11904228, 11804221, and 11655002), the National Postdoctoral Program for Innovative Talents of China (Grant No. BX201700156), and the Science and Technology Commission of Shanghai Municipality, China (Grant No. 16DZ2260200).

†Corresponding author. E-mail: panjsong@gmail.com

‡Corresponding author. E-mail: wvliu@pitt.edu

© 2021 Chinese Physical Society and IOP Publishing Ltd

$$+z\Big(-\frac{\nabla^2}{4m}\Big)^2-\mu_{\rm M}\Big)\hat{\phi}_m-\bar{g}(\hat{\phi}_m^\dagger y_m+{\rm h.c.})\Big]+\mathcal{H}_{\rm bg}, \quad (1)$$

where the operator y_m and background interaction $\mathcal{H}_{\rm bg}$ are respectively given by

$$\begin{aligned} y_m &= \frac{1}{4}\sum_{a,b=x,y,z} C_{ab}^m\big[(\partial_a\hat{\psi}_1)(\partial_b\hat{\psi}_2)-(\partial_a\partial_b\hat{\psi}_1)\hat{\psi}_2 \\ &\quad +(\partial_b\hat{\psi}_1)(\partial_a\hat{\psi}_2)-\hat{\psi}_1(\partial_a\partial_b\hat{\psi}_2)\big], \quad (2) \\ \mathcal{H}_{\rm bg} &= \frac{1}{2}\sum_{\sigma,\sigma'=1,2}\lambda_{\sigma\sigma'}|\hat{\psi}_\sigma|^2|\hat{\psi}_{\sigma'}|^2+\sum_{m,n=-2}^{2}\frac{g_0}{2}(\hat{\phi}_m^\dagger\hat{\phi}_m)(\hat{\phi}_n^\dagger\hat{\phi}_n) \\ &\quad +\sum_{m=-2}^{2} g_{\rm AM}(|\hat{\psi}_1|^2+|\hat{\psi}_2|^2)\hat{\phi}_m^\dagger\hat{\phi}_m. \quad (3) \end{aligned}$$

Here, μ_1, μ_2, and $\mu_{\rm M}$ are the chemical potentials of the atoms and the molecule, respectively. The detuning between the atomic and molecular channels is given by $\nu=\mu_1+\mu_2-\mu_{\rm M}$. $\bar{g}$ denotes the d-wave's interaction strength. C_{ab}^m is the Clebsch–Gordan coefficient,[11] satisfying $\sum_{a,b}C_{ab}^m k_a k_b/k^2=\sqrt{4\pi}Y_2^m(\hat{k})$, where $Y_2^m(\hat{k})$ are the spherical harmonics of degree 2 arising from the d-wave components of two-body wave function. For simplicity, we have taken the two atomic masses m to be identical, which is a good approximation for mixtures of isotopes such as ^{85}Rb and ^{87}Rb. Thus, the molecules have the mass of $2m$. The z term in Eq. (1) is formally introduced to normalize the d-wave interaction,[12] but it does not actually affect the mean-field dynamics. In the background interaction $\mathcal{H}_{\rm bg}$, the $\lambda_{\sigma\sigma'}$ term characterizes the atom–atom interactions caused by different species, the $g_{\rm AM}$ term describes the atom–molecule interaction, and the g_0 term describes the molecule–molecule interaction. We restrict ourselves to the homogeneous case for simplicity and clarity, adopting the local density approximation (widely applied to the study of trapped gases) used in the experiment. It proved to be a good approximation for a slowly varying trap potential with a large number of atoms in the experiment.

3. Mean-field theory

We will obtain the Landau free energy by applying mean-field theory to our model and minimize it to establish the phase diagram and analyze the phase transition. This method is equivalent to solving the Gross–Pitaevskii equation. Replacing the atomic and molecular field operators with their relative classical order parameters Ψ_σ, Φ_m, we obtain the Landau free-energy function $F[\Psi_\sigma,\Phi_m]=\langle H\rangle$.

We decompose our mean-field parameters to characterize the states of the system. For the atomic condensates Ψ_1 and Ψ_2, let us use a Fourier transform and make these fields complex periodic functions characterized by momenta Q_n,

$$\Psi_\sigma=\sum_{Q_n}\Psi_{\sigma,Q_n}e^{iQ_n\cdot r}. \quad (4)$$

It is generally expected that if a single component is assumed, $Q_n=Q$ it is sufficient to capture the qualitative picture of the ground state.[13] Unlike the p-wave case,[7] the d-wave interaction is proportional to the square of the momentum and thus cannot give rise to finite-momentum molecular condensates, since the minimum of the total energy remains at the zero momentum of the molecules. To conserve momentum, the ground state should fall into one of two universal classes: the FF (Fulde–Ferrell)-like[14] form $\Psi_\sigma^{\rm FF}=\Psi_{\sigma,Q_\sigma}e^{iQ_\sigma\cdot r}$ or the LO (Larkin–Ovchinnikov)-like[15] form $\Psi_\sigma^{\rm LO}=\Psi_{\sigma,Q}e^{iQ\cdot r}+\Psi_{\sigma,-Q}e^{-iQ\cdot r}$, where $\Psi_{\sigma,Q}=\Psi_{\sigma,-Q}$. Based on an analysis of the total energy (see supplementary), the order parameters favor the simplest but non-trivial FF-like form with a single ordering wavevector $Q_1=-Q_2=Q$, described by

$$\begin{aligned} \Psi_1 &= \Psi_{1,Q}e^{iQ\cdot r}, \\ \Psi_2 &= \Psi_{2,-Q}e^{-iQ\cdot r}. \end{aligned} \quad (5)$$

3.1. Atomic superfluid phase

For large positive detuning $\nu>0$, the atomic channels have lower energy and the ground state is a molecule vacuum. The free energy is minimized by spatially uniform atomic order parameters[16] and leads to a free energy density of the form

$$f_A=-\sum_{\sigma=1,2}\mu_\sigma|\Psi_\sigma|^2+\sum_{\sigma,\sigma'=1,2}\frac{\lambda_{\sigma,\sigma'}}{2}|\Psi_\sigma|^2|\Psi_{\sigma'}|^2. \quad (6)$$

For $4\lambda_{11}\lambda_{22}-(\lambda_{12}+\lambda_{21})^2>0$, the minimization of f_A leads to different superfluid phases as μ_1 and μ_2 change, which are listed in Table 1 (see Fig. 1). Otherwise, for $4\lambda_{11}\lambda_{22}-(\lambda_{12}+\lambda_{21})^2<0$, the $\rm ASF_{12}$ phase tends to be unstable, there will be a direct first-order phase transition from $\rm ASF_1$ to $\rm ASF_2$, and its phase boundary is determined to be $\mu_2=\sqrt{\frac{\lambda_{22}}{\lambda_{11}}}\mu_1$ (see Fig. 2).

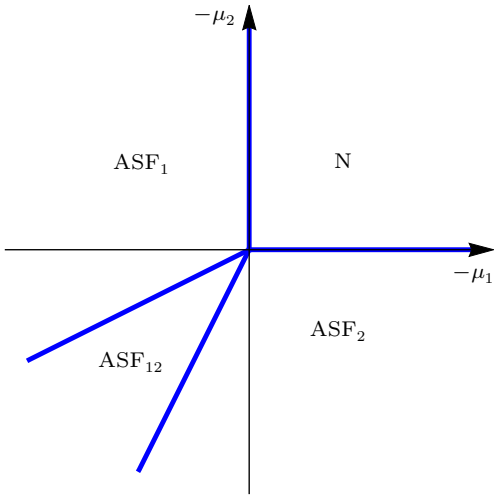


Fig. 1. Mean-field phase diagram of a d-wave resonant two-component Bose gas with a large positive detuning and $4\lambda_{11}\lambda_{22}-(\lambda_{12}+\lambda_{21})^2>0$. The atomic channels have lower energy. $\rm ASF_1$ and $\rm ASF_2$ refer to single-atom species' superfluid states, and $\rm ASF_{12}$ refers to a double-atom species's superfluid state.

Table 1. Sub-phases of the ASF phase. (i) When μ_1 and μ_2 are negative, both atomic species are in the normal (N) phase. (ii) When $\mu_1 > 0$, $\mu_2 < \frac{\lambda_{12}+\lambda_{21}}{2\lambda_{11}}\mu_1$, atom 1 forms a condensate. (iii) When $\mu_1 < \frac{\lambda_{12}+\lambda_{21}}{2\lambda_{22}}\mu_2$, $\mu_2 > 0$, atom 2 a forms condensate. (iv) When $\mu_1 > \frac{\lambda_{12}+\lambda_{21}}{2\lambda_{22}}\mu_2$, $\mu_2 > \frac{\lambda_{12}+\lambda_{21}}{2\lambda_{11}}\mu_1$, both atom species form condensates.

Phase	Chemical potentials	Ψ_1	Ψ_2
N	$\mu_1 < 0,\ \mu_2 < 0$	0	0
ASF_1	$\mu_1 > 0,\ \mu_2 < \frac{\lambda_{12}+\lambda_{21}}{2\lambda_{11}}\mu_1$	$\sqrt{\frac{\mu_1}{\lambda_{11}}}$	0
ASF_2	$\mu_1 < \frac{\lambda_{12}+\lambda_{21}}{2\lambda_{22}}\mu_2,\ \mu_2 > 0$	0	$\sqrt{\frac{\mu_2}{\lambda_{22}}}$
ASF_{12}	$\mu_1 > \frac{\lambda_{12}+\lambda_{21}}{2\lambda_{22}}\mu_2,\ \mu_2 > \frac{\lambda_{12}+\lambda_{21}}{2\lambda_{11}}\mu_1$	$\sqrt{\frac{4\lambda_{22}\mu_1 - 2(\lambda_{12}+\lambda_{21})\mu_2}{4\lambda_{11}\lambda_{22}-(\lambda_{12}+\lambda_{21})^2}}$	$\sqrt{\frac{4\lambda_{11}\mu_2 - 2(\lambda_{12}+\lambda_{21})\mu_1}{4\lambda_{11}\lambda_{22}-(\lambda_{12}+\lambda_{21})^2}}$

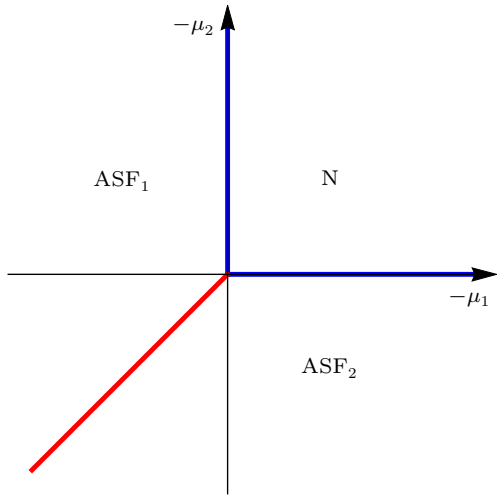


Fig. 2. Mean-field phase diagram of a d-wave resonant two-component Bose gas with large positive detuning and $4\lambda_{11}\lambda_{22} - (\lambda_{12}+\lambda_{21})^2 < 0$. A valid phase of the significant condensate fraction in both atomic fields is not found by mean-field calculation. The phases ASF_1 and ASF_2 are separated by a first-order transition boundary.

3.2. Molecular superfluid phase

In the MSF phase, there is large negative detuning $\nu < 0$, that is, $-\nu \gg |\mu_{1,2}|$. The molecular channels have lower energy and the ground state is an atomic vacuum. The free energy density f_{M} is given as

$$f_{\mathrm{M}} = \sum_{m=-2}^{2} -\mu_{\mathrm{M}}|\Phi_m|^2 + \sum_{m,n=-2}^{2}\frac{g_0}{2}(\Phi_m^*\Phi_m)(\Phi_n^*\Phi_n). \quad (7)$$

The molecular condensate density is obtained by minimizing the free energy

$$\Phi = \sqrt{\frac{\mu_{\mathrm{M}}}{g_0}}D(0,0,1,0,0)^{\mathrm{T}}, \quad (8)$$

where D is an $SU(5)$ matrix satisfying $D\cdot D^{\dagger} = 1$. The ground state implies a broken symmetry group $SU(5)$.

3.3. Atomic–molecular superfluid

For intermediate detuning, both the atomic and molecular modes are gapless. To understand the phase boundaries and the behavior of the order parameters, it is convenient to approach the AMSF phase by starting from the MSF phase.[7] For simplicity, we specialize in a balanced mixture, where $\mu_1 = \mu_2 = \mu$. Applying the mean-field assumption, we obtain the free energy density $f_{\mathrm{AM}} = F[\Psi_\sigma, \Phi_m]/V = f_Q + f_{\mathrm{M}}$, where f_Q describes the Q-dependent portion of the free energy density f_{AM},

$$f_Q = \sum_{\sigma=1,2}\varepsilon_Q|\Psi_{\sigma,Q_\sigma}|^2 - (\Delta_Q^*\Psi_{1,Q}\Psi_{2,-Q} + \mathrm{c.c.}) + \sum_{\sigma,\sigma'=1,2}\frac{\lambda_{\sigma,\sigma'}}{2}|\Psi_{\sigma,Q_\sigma}|^2\left|\Psi_{\sigma',Q_{\sigma'}}\right|^2, \quad (9)$$

$$f_{\mathrm{M}} = -\sum_{m=-2}^{2}\mu_{\mathrm{M}}\Phi_m^*\Phi_m + \sum_{m,n=-2}^{2}\frac{g_0}{2}(\Phi_m^*\Phi_m)(\Phi_n^*\Phi_n). \quad (10)$$

In the above equations, the atomic order parameter ansatz Eq. (5) is used to simplify f_Q. Also, $\varepsilon_Q = (\frac{Q^2}{2m} - \mu + \sum_{m=-2}^{2} g_{\mathrm{AM}}|\Phi_m|^2)$, $\Delta_Q = \sum_{m=-2}^{2}\bar{g}\sqrt{4\pi}Q^2Y_2^m(\hat{Q})\Phi_m$, $Q_1 = Q$ and $Q_2 = -Q$. When we approach the ASMF phase from the MSF phase, the atomic condensate fractions are considered to be small and perturbative. Thus, the quadratic order terms are sufficient to characterize the free energy density f_Q. Besides, when an atomic condensate is emergent in the AMSF phase, it prefers to stay at a lower energy level. The condensate mean-field ground states are obtained by minimizing the free energy f_{AM}

$$Q = 0, \quad (11)$$

$$\Phi = \sqrt{\frac{g_{\mathrm{AM}}\mu - \lambda\mu_{\mathrm{M}}}{g_{\mathrm{AM}}^2 - g_0\lambda}}D(0,0,1,0,0)^{\mathrm{T}}, \quad (12)$$

$$|\Psi_{1,2}| = \sqrt{\frac{g_0\mu - g_{\mathrm{AM}}\mu_{\mathrm{M}}}{2\lambda g_0 - 2g_{\mathrm{AM}}^2}}, \quad (13)$$

where D is an $SU(5)$ rotation matrix. Similarly to the analysis in the MSF context, the broken symmetry group is $SU(5)$. It is worth noting that a zero-momentum solution is needed to minimize the free energy, which is different from the finite momentum case that applies to p-wave interaction gases.[7] The condensate densities are

$$n_{\mathrm{M}} = \frac{(2\lambda - g_{\mathrm{AM}})\mu - \lambda\nu}{\lambda g_0 - g_{\mathrm{AM}}^2}, \quad (14)$$

$$n_{\mathrm{A}} = \frac{(g_0 - 2g_{\mathrm{AM}})\mu + g_{\mathrm{AM}}\nu}{\lambda g_0 - g_{\mathrm{AM}}^2}. \quad (15)$$

By setting $n_{\rm A}=0$ and $n_{\rm M}=0$, respectively, we obtain the two phase boundaries that separate the three phases, the molecular superfluid (MSF) phase, the atomic–molecular superfluid (AMSF) phase, and the atomic superfluid (ASF) phase.

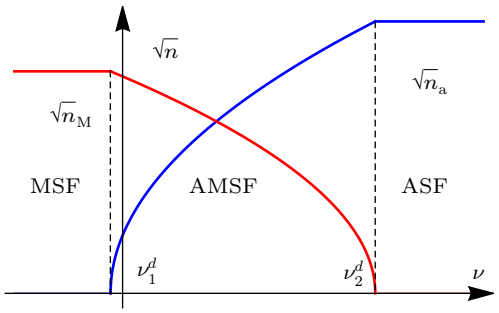


Fig. 3. Atomic and molecular condensate density versus FR detuning ν. The red curves denote the molecular condensate density, the blue curves denote the atomic condensate density. (i) MSF for $\nu<\nu_1^d$; (ii) AMSF for $\nu_1^d<\nu<\nu_2^d$; (iii) ASF for $\nu>\nu_2^d$.

The relation between the condensate densities and the detuning is depicted in Fig. 3,

$$\nu_1^d=\Big(2-\frac{g_0}{g_{\rm AM}}\Big)\mu, \tag{16}$$

$$\nu_2^d=\Big(2-\frac{g_{\rm AM}}{\lambda}\Big)\mu. \tag{17}$$

4. Low energy excitations

In this section, we will focus on low-energy excitation of the d-wave FR to double-check the consistency of the mean-field results. To begin with, we expand the field operators in the ASF, MSF, and AMSF phases around their mean-field condensate values,[7,8] $\hat{\psi}_\sigma=\Psi_\sigma+\delta\hat{\psi}_\sigma$ and $\hat{\phi}_m=\Phi_m+\delta\hat{\phi}_m$. With these perturbation field representations, the Hamiltonian (1) is expanded up to the second order in the momentum space with creation and annihilation operators $\hat{a}_{\sigma,k}$ and $\hat{b}_{m,k}$,

$$\begin{aligned}H_f=&\sum_k\Bigg\{\sum_{\sigma=1,2}\Big(\frac{1}{2}\varepsilon_{\sigma,k+Q_\sigma}\hat{a}^\dagger_{\sigma,k+Q_\sigma}\hat{a}_{\sigma,k+Q_\sigma}+\tilde{\lambda}_\sigma\hat{a}_{\sigma,-k+Q_\sigma}\hat{a}_{\sigma,k+Q_\sigma}\Big)+t_1\hat{a}^\dagger_{1,k+Q}\hat{a}_{2,k-Q}+t_{2,k+Q}\hat{a}_{1,k+Q}\hat{a}_{2,-k-Q}\\&+\sum_m\Big(\frac{1}{2}\omega_{m,k}\hat{b}^\dagger_{m,k}\hat{b}_{m,k}+\delta_m\hat{b}_{m,-k}\hat{b}_{m,k}\Big)+\frac{1}{2}\sum_{m\neq n}\Big(g_{m,n}\hat{b}^\dagger_{n,k}\hat{b}_{m,k}+\gamma_{m,n}\hat{b}_{m,-k}\hat{b}_{n,k}\Big)+\sum_{\sigma,m}\beta_{1,m,\sigma}\hat{a}^\dagger_{\sigma,k+Q_\sigma}\hat{b}_{m,k}\\&+\sum_{\sigma,m}\beta_{2,m,\sigma}\hat{a}^\dagger_{\sigma,k+Q_\sigma}\hat{b}^\dagger_{m,-k}+\sum_{\sigma,m}\beta_{3,m,\sigma}\hat{a}_{\sigma,-k+Q_\sigma}\hat{b}_{m,k}+\sum_{\sigma,m}\beta_{4,m,\sigma}\hat{a}_{\sigma,-k+Q_\sigma}\hat{b}^\dagger_{m,-k}-\sum_{\sigma,m}\alpha_{m,\overline{\sigma},k}\hat{b}^\dagger_{m,k}\hat{a}_{\sigma,k+Q_\sigma}+\text{h.c.}\Bigg\}.\end{aligned} \tag{18}$$

The parameters are defined below:

$$\begin{aligned}\varepsilon_{\sigma,k}&=\varepsilon_k-\mu_\sigma+2\lambda_{\sigma,\sigma}|\Psi_\sigma|^2+\frac{1}{2}(\lambda_{12}+\lambda_{21})|\Psi_{\overline{\sigma}}|^2\\&\quad+g_{\rm AM}\sum_m\Phi^*_m\Phi_m,\end{aligned} \tag{19}$$

$$\begin{aligned}\omega_{m,k}&=\frac{1}{2}\varepsilon_k+z\Big(\frac{1}{2}\varepsilon_k\Big)^2-\mu_{\rm M}+g_0\sum_n\Phi^*_n\Phi_n\\&\quad+g_0\Phi^*_m\Phi_m+g_{\rm AM}(|\Psi_1|^2+|\Psi_2|^2),\end{aligned} \tag{20}$$

$$\widetilde{\lambda}_\sigma=\frac{1}{2}\lambda_{\sigma,\sigma}\Psi^{*2}_\sigma, \tag{21}$$

$$t_1=\frac{1}{2}(\lambda_{12}+\lambda_{21})\Psi_1\Psi^*_2, \tag{22}$$

$$t_{2,k}=\frac{1}{2}(\lambda_{12}+\lambda_{21})\Psi^*_1\Psi^*_2-\overline{g}\sqrt{4\pi}k^2\sum_m\Phi^*_mY^m_2(\hat{k}), \tag{23}$$

$$\delta_m=\frac{1}{2}g_0\Phi^*_m\Phi^*_m, \tag{24}$$

$$g_{m,n}=g_0\Phi^*_m\Phi_n, \tag{25}$$

$$\gamma_{m,n}=g_0\Phi^*_m\Phi^*_n, \tag{26}$$

$$\beta_{1,m,\sigma}=g_{\rm AM}\Psi_\sigma\Phi^*_m, \tag{27}$$

$$\beta_{2,m,\sigma}=g_{\rm AM}\Psi_\sigma\Phi_m, \tag{28}$$

$$\beta_{3,m,\sigma}=g_{\rm AM}\Psi^*_\sigma\Phi^*_m, \tag{29}$$

$$\beta_{4,m,\sigma}=g_{\rm AM}\Psi^*_\sigma\Phi_m, \tag{30}$$

$$\alpha_{m,\sigma,k}=\overline{g}\sqrt{4\pi}\Psi_{\sigma,Q_\sigma}\Big(Q_\sigma-\frac{k}{2}\Big)^2Y^m_2(\widehat{k-2Q_\sigma}), \tag{31}$$

where $\varepsilon_k=\frac{k^2}{2m}$, $\overline{1}=2$ and $\overline{2}=1$. The Hamiltonian is theoretically diagonalized up to the k^2-th order, and an exact diagonalization is used to validate our analysis in the meanwhile.

4.1. Atomic superfluid

In the ASF phase, the previous section confirmed that the molecular modes are gapped. The relative mean field $\Phi_m=0$, and the atoms are condensed at zero momentum $Q=0$. To discover the atomic modes, we need to integrate the molecular modes out (see Supplementary). In the low-energy regime, when $k\to0$, we calculate the dispersion up to the k^2-th order. The atomic and molecular modes are given by

$$E^{\rm A}_{1,k}=\sqrt{\frac{k^2}{2m}\Big(\frac{k^2}{2m}+2\lambda n_{\rm A}\Big)}, \tag{32}$$

$$E^{\rm A}_{2,k}=\sqrt{\frac{(2\lambda-\lambda_{12}-\lambda_{21})n_{\rm A}}{2m}}k, \tag{33}$$

$$E^{\rm M}_{-2,-1,0,1,2,k}=\frac{k^2}{4m}+\nu-2\lambda n_{\rm A}+g_{\rm AM}n_{\rm A}, \tag{34}$$

where $n_{\rm A}$ is the atomic condensate density at the mean-field level, $n_{\rm A}=|\Psi_1|^2+|\Psi_2|^2$. The atomic modes are gapless excitations in the superfluid states. The molecular modes have an energy gap given by $\nu-2\lambda n_{\rm A}+g_{\rm AM}n_{\rm A}$. When it vanishes, we have a transition from the ASF phase to the AMSF phase at the detuning value

$$\nu=2\lambda n_{\rm A}-g_{\rm AM}n_{\rm A}, \tag{35}$$

which is consistent with Eq. (17) ($n_{\rm A}=\mu/\lambda$). Figure 4 shows the theoretical and numerical results. They are a good fit for the small-k region.

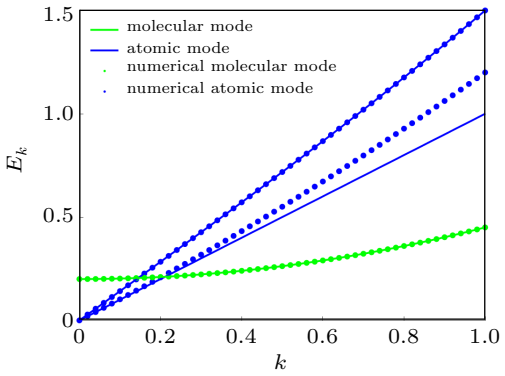


Fig. 4. ASF phase excitation spectrum. Here, we use the parameters $\{m=1,\mu=1,\nu=3.2,\lambda_{11}=\lambda_{22}=3,\lambda_{12}=\lambda_{21}=1\}$. The units are arbitrary. All the molecular modes are gapped, but the atomic modes are gapless. The five molecular modes are degenerate. The numerical and theoretical results are a good fit for the small-k regime.

4.2. Molecular superfluid

In the MSF phase, the atomic modes are gapped and their mean fields $\Psi_1=\Psi_2=0$. The vanishment of the atomic mean fields results in $\alpha_{m,\sigma,k}=0$, which means that the atomic Hamiltonian and the molecular Hamiltonian are separable (see supplementary). Referring to the mean-field ground state (8), we choose the simplest case, $D=1$, to explore its low-energy excitation, and it leads to $\Phi_{-2,-1,1,2}=0$, $\Phi_0=\sqrt{n_{\rm M}}$. The respective atomic dispersions are degenerate,

$$E_k^{\rm A}=\sqrt{\varepsilon_k^2-4\pi\bar{g}^2k^4\sum_{m,n}\Phi_m Y_2^m(\hat{k})\Phi_n^* Y_2^n(\hat{k})}, \tag{36}$$

$$E_{0,k}^{\rm M}=\sqrt{\frac{g_0 n_{\rm M}}{2m}}k, \tag{37}$$

$$E_{n=\pm1,\pm2,k}^{\rm M}=\frac{k^2}{4m}. \tag{38}$$

The five molecular modes are all gapless, which proves that they are in a superfluid state. For the MSF phase, $\mu=\frac{1}{2}(\mu_{\rm M}+\nu)<\frac{1}{2}(\mu_{\rm M}+\nu_1^d)$, from which we can obtain $-\mu+g_{\rm AM}n_{\rm M}>0$.

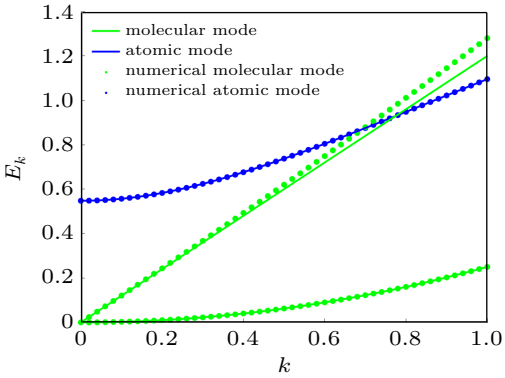


Fig. 5. MSF phase-excitation spectrum. The parameters used for the MSF phase are $\{m=1,\mu=0,\nu=-1.44,g_0=1\}$. The units are arbitrary. The atomic modes are gapped and degenerate. All the molecular modes are gapless; $m=\pm1,\pm2$ are degenerate and denoted by the lower green line, and $m=0$ is denoted by the upper green line.

Therefore, in Eq. (36) $k=0$ yields the energy gap,

$$\Delta E_k^{\rm A}=-\mu+g_{\rm AM}n_{\rm M}. \tag{39}$$

By setting $\Delta E_k^{\rm A}=0$, the atomic modes become gapless and the atomic condensates are emergent. Applying $\nu=2\mu-\mu_{\rm M}$ and $\mu_{\rm M}=g_0n_{\rm M}$ (see Eq. (8)), we obtain the transition from the MSF phase to the AMSF phase at the detuning value

$$\nu=\left(2-\frac{g_0}{g_{\rm AM}}\right)\mu, \tag{40}$$

which is consistent with Eq. (16). Figure 5 shows the consistency between the theoretical and numerical results.

4.3. Atomic–molecular superfluid

For the intermediate phase, both atomic and molecular condensates exist. Hence, they define a complicated coupled Hamiltonian (see supplementary). The molecular and atomic condensate mean-field solutions are given by

$$\Phi=\sqrt{\frac{g_{\rm AM}\mu-\lambda\mu_{\rm M}}{g_{\rm AM}^2-g_0\lambda}}D(0,0,1,0,0)^{\rm T}, \tag{41}$$

$$\Psi_{1,2}=\sqrt{\frac{g_0\mu-g_{\rm AM}\mu_{\rm M}}{2\lambda g_0-2g_{\rm AM}^2}}. \tag{42}$$

Similarly to what we achieved in the MSF phase, we choose the simplest case to compute the spectra, $D=1$. Diagonalizing this Hamiltonian yields the spectra up to the k-th order

$$E_{1,k}^{\rm A}=\sqrt{\frac{\lambda n_{\rm A}}{m}}k, \tag{43}$$

$$E_{2,k}^{\rm A}=\sqrt{(2\lambda-\lambda_{12}-\lambda_{21})n_{\rm A}\left(\frac{1}{2m}-\sqrt{5n_{\rm M}\bar{g}}\right)}k, \tag{44}$$

$$E_{0,k}^{\rm M}=\sqrt{\frac{\left(g_0+\frac{g_{\rm AM}^2}{\lambda}\right)n_{\rm M}}{2m}}k, \tag{45}$$

$$E_{n=\pm1,\pm2,k}^{\rm M}=\frac{k^2}{4m}. \tag{46}$$

Figure 6 shows the consistency between the theoretical results and numerical results.

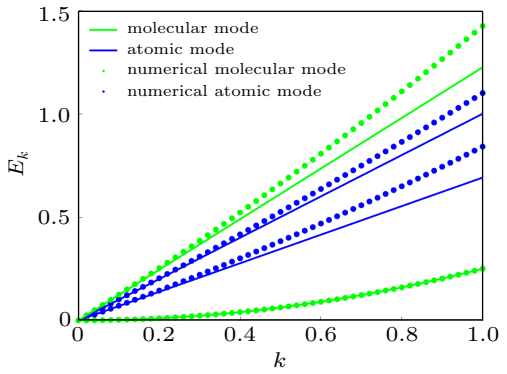


Fig. 6. AMSF phase-excitation spectrum. The parameters here are: $\{m=1,\mu=0,\nu=-1,\lambda_{11}=\lambda_{22}=1.5,\lambda_{12}=\lambda_{21}=0.5,g_0=2,g_{\rm AM}=-1,\bar{g}=0.01\}$. The units are arbitrary. The atomic modes are gapless for the two blue lines. The molecular modes are also gapless: $m=\pm1,\pm2$ are degenerate and denoted by the lower green line; $m=0$ is denoted by the upper green line.

5. Final remarks and conclusions

In general, atomic loss is inevitable near a Feshbach resonance. In this case, the free energy becomes complex and the ground states are no longer stable. For simplicity, let us qualitatively estimate the effect of atomic loss by introducing imaginary parts into the chemical potentials $\mu_{1,2,\mathrm{M}}$. However, as a criterion, different quantum phases may be straightforwardly obtained from Table 1 by replacing the chemical potentials with their real parts, if we determine the ground states according to the real parts of the free energies in Eqs. (6), (8), (9), and (10). The imaginary parts of the free energies determine the damping rates of the corresponding ground states. When the relaxation times (to the equilibrium states) are far shorter than the lifetime of the atomic gas due to atomic loss, the ground states predicted here are still observable. The qualitative properties of low-energy excitation spectra (such as the numbers of gapless modes) are also expected to be unchanged due to the introduction of atomic loss when the continuous symmetries are not broken. It is hard to quantitatively estimate the effect of atomic loss at this stage, since the experiment lacks the necessary data.

In this paper, we studied the mean-field ground state of a d-wave interacting Bose gas, and found that there are three superfluid phases: the atomic, molecular and atomic–molecular superfluid phases. What was most surprising was that, unlike the p-wave case,[7–9] we found that the atomic superfluid does not carry finite momentum. Furthermore, we studied the low-energy excitation spectrum above the superfluid phases. Our work provides a basic reference for experiments on degenerate d-wave interacting Bose gases.

Acknowledgment

The authors are indebted to Bing Zhu and Chao Gao for helpful discussion.

References

[1] Chin C, Grimm R, Julienne P and Tiesinga E 2010 *Rev. Mod. Phys.* **82** 1225
[2] Beaufils Q, Crubellier A, Zanon T, Laburthe-Tolra B, Maréchal E, Vernac L and Gorceix O 2009 *Phys. Rev. A* **79** 032706
[3] Cui Y, Shen C Y, Deng M, Dong S, Chen C, Lü R, Gao B, Tey M K and You L 2017 *Phys. Rev. Lett.* **119** 203402
[4] Werner J, Griesmaier A, Hensler S, Stuhler J, Pfau T, Simoni A and Tiesinga E 2005 *Phys. Rev. Lett.* **94** 183201
[5] Yao X C, Qi R, Liu X P, Wang X Q, Wang Y X, Wu Y P, Chen H Z, Zhang P, Zhai H, Chen Y A and Pan J W 2019 *Nat. Phys.* **15** 570
[6] Zhu B, Häfner S, Tran B, Gerken M, Ulmanis J, Tiemann E and Weidemüller M 2019 arXiv:1912.01264v1 [cond-mat.quant-gas]
[7] Choi S and Radzihovsky L 2011 *Phys. Rev. A* **84** 043612
[8] Li Z H, Pan J S and Liu V W 2019 *Phys. Rev. A* **100** 053620
[9] Radzihovsky L and Choi S 2009 *Phys. Rev. Lett.* **103** 095302
[10] Yao X C, Qi R, Liu X P, Wang X Q, Wang Y X, Wu Y P, Chen H Z, Zhang P, Zhai H, Chen Y A *et al.* 2017 arXiv:1711.06622v1 [cond-mat.quant-gas]
[11] Yao J and Zhang S Z 2018 *Phys. Rev. A* **97** 043612
[12] Zhang P F, Zhang S Z and Yu Z H 2018 *Phys. Rev. A* **95** 043609
[13] Kuklov A B 2006 *Phys. Rev. Lett.* **97** 110405
[14] Fulde P and Ferrell R 1964 *Phys. Rev.* **135** A550
[15] Larkin A and Ovchinnikov Y 1965 *Sov. Phys. JETP* **20** 762
[16] Calabrese P, Pelissetto A and Vicari E 2003 *Phys. Rev. B* **67** 054505